

Observations of a Phenomenal Temperature Perturbation in Tropical Cyclone Kerry (1979)

GREG J. HOLLAND¹

Department of Atmospheric Science, Colorado State University, Fort Collins, CO 80521

THOMAS D. KEENAN

Bureau of Meteorology, Melbourne, Australia

GEOFF D. CRANE

Bureau of Meteorology, Brisbane, Australia

(Manuscript received 3 January 1983, in final form 1 February 1984)

ABSTRACT

Observations are presented of a phenomenal upper tropospheric mesoscale temperature perturbation arising from the interaction between dissipating Tropical Cyclone Kerry (1979) and a midlatitude trough in the westerlies, which we describe as a black hole from its appearance on satellite imagery. We propose that this perturbation arose from dynamically forced subsidence along a confluence between the environmental flow and outflow from a major convective complex. The frequency of occurrence and subsequent adjustment of the atmosphere is described and discussed.

1. Introduction

Tropical Cyclone Kerry was in the final stages of dissipation on 4 March 1979 when a Qantas Boeing 747 jet, returning to Brisbane on a routine commercial flight from Port Moresby at 230 mb, passed just east of the eye then deviated to the west to fly around a line of deep convection extending into the southern quadrant of the cyclone. As the aircraft passed the downstream end of the convective line, it encountered a phenomenal increase in air temperature; the temperature rose 18 K in 60 km and returned to ambient values again in just 13 km!

It is unlikely that this observation was an instrument error or exaggeration. The aircraft instrumentation consisted of a Rosemont probe with a maximum read-out error of ± 1.3 K. The entire sequence of events was also recorded by the third author, who is an experienced tropical cyclone forecaster. He reported that the jet engines (which are very sensitive to air temperature) lost considerable power and, at the same time, the air speed fell alarmingly. We shall also show that satellite and other data support this observation.

In this paper, we document the available observations around the cyclone at this time. We further suggest that the observed temperature increase resulted from a dynamic interaction between a midlatitude

trough and the deep convection to the south of the cyclone. In particular, we propose that a complex of convective elements penetrating into the stratosphere set up a perturbation on the tropopause; dynamic interaction then occurred with the westerly flow around the midlatitude trough to produce a rapid downward advection of stratospheric air. This process, its energetics and the subsequent adjustment of the atmosphere are described and discussed.

2. Synoptic history

Tropical Cyclone Kerry formed to the east of the Solomon Islands in mid-February 1979 and, as shown in Fig. 1, moved on an erratic path through the Coral Sea to landfall on the Australian coast near Mackay on 1 March. Further details of this long and interesting life cycle may be found in Broadbridge (1981) and Sheets and Holland (1981). Our interest centers on the subsequent northward movement and reintensification of the cyclone off Townsville on 3 March, followed by a rapid southeastward movement and dissipation under the influence of a mobile midlatitude trough on 4 and 5 March. This interaction with, as well as destruction by the midlatitude trough is well shown by the sequences of 250 mb synoptic analyses in Fig. 2.

On 4 March, the cyclone was well into its dissipating stage. At 0600 GMT the GMS (Geostationary Mete-

¹ Permanent affiliation: Bureau of Meteorology, Melbourne.

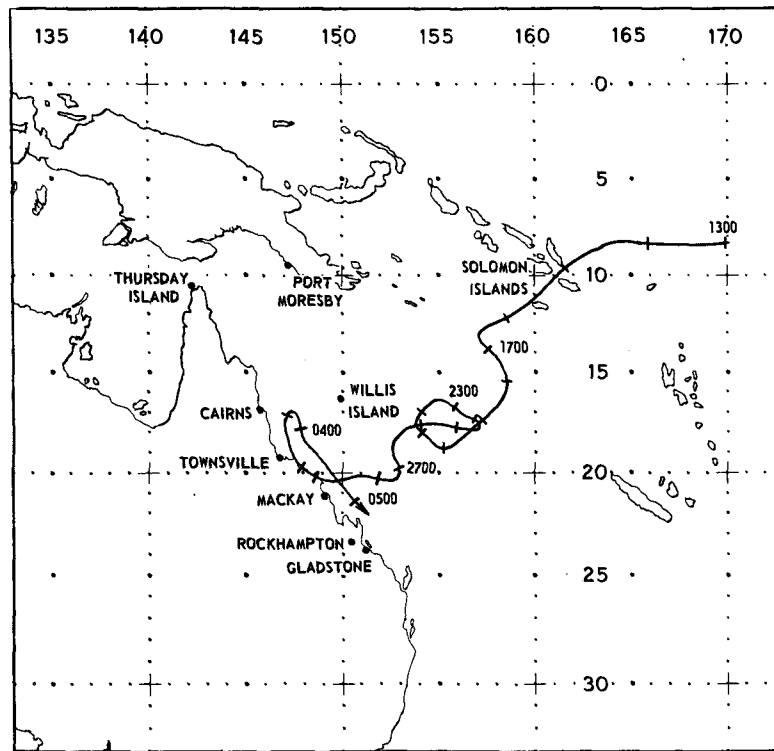


FIG. 1. Track of Tropical Cyclone Kerry, 13 February–5 March 1979. Ticks give successive 0000 GMT (about 0900 LST) positions. (Code 1700 represents 17 February 0000 GMT.)

orological Satellite) imagery (Fig. 3) showed a ragged, highly asymmetric system with only a semblance of an eye and convection concentrated in the eastern and southeastern sectors. (Note, however, the evidence of very deep penetrative convection in this region.) As can be seen in Fig. 2, the trough was orientated north-west–southwest along the Australian coast and a deep layer of westerly flow existed above 500 mb. The low-level wind field in Kerry's vicinity, as shown by the analysis of reconnaissance observations by a U.S. NOAA Lockheed WP-3D Orion research aircraft in Fig. 4, indicates near hurricane force winds on the eastern side with a secondary maximum in a confluence band 700–100 km from the center and extending from the east around to the south of the cyclone.

3. Observations

The Qantas 747's track at flight level 370 (about 230 mb) with superimposed wind and temperature observations is shown in Fig. 5, together with a streamline analysis and a schematic of the PPI (Plan Position Indicator) from the Townsville WF44 10 cm radar for 0700 (all times GMT) 4 March. The diversion to the right of the planned flight path was to avoid severe weather at the downstream end of the convective band. Note the cyclonic turning of the winds, but no tem-

perature change, as the aircraft traversed to the east of the eye. This was followed by an 18 K temperature increase in an easterly flow downstream of the convective band, then a rapid return to ambient temperature as the aircraft crossed a sharp anticyclonic wind shear and entered the zone of midlatitude westerlies. The observed ambient temperatures agreed very well with those reported by radiosonde flights at Townsville and Willis Island. Also plotted in Fig. 5 are observed 200 mb winds from rawin flights at Townsville, Cairns, Willis Island and Mackay; again, the aircraft observations agree quite well.

Note also that the convective band radar return ends abruptly in an almost square cutoff on the downstream end. This is confirmed by the visible satellite imagery for 0600 in Fig. 3, a schematic of which is shown in Fig. 6. We further note the convective complex to the south of the cyclone eye. This complex, which was the cause of the aircraft's diversion, contained convective elements which were penetrating through the upper stable layer—possibly into the stratosphere. Further downstream, the cirrus ends sharply with a "black hole", or clear region, coinciding with the observed mesoscale temperature perturbation. To the west of this region is a single long cirrus line which appears to coincide with the zone of convergent easterly and westerly flow. As we shall discuss in the following sec-

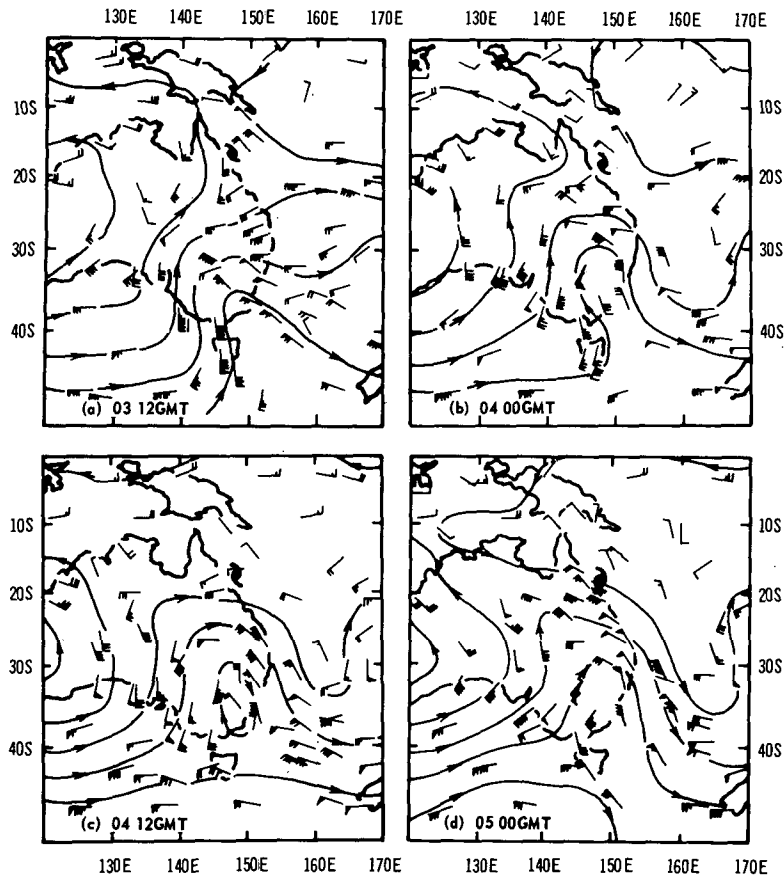


FIG. 2. Sequence of 250 mb, synoptic scale streamline analyses from 1200 on 3 March to 0000 on 5 March, showing the interaction between Tropical Cyclone Kerry and the midlatitude trough. Each full wind barb represents 5 m s^{-1} . All times are GMT.

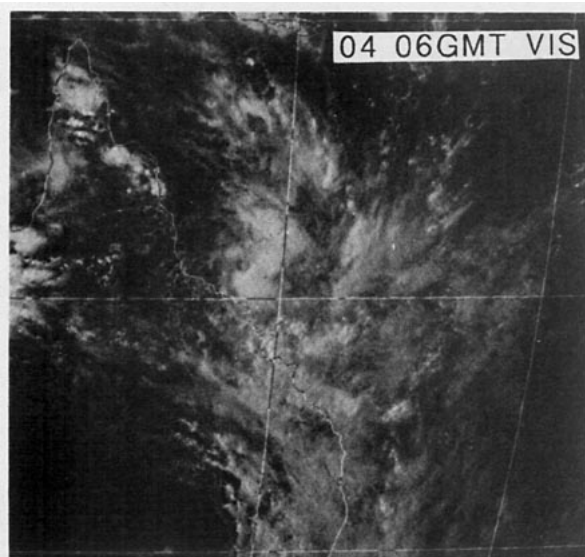


FIG. 3. GMS imagery of Tropical Cyclone Kerry at 0600 on 4 March.

tion, an important feature of the interaction was the rapid growth of the convective complex to the south of Kerry which occurred concomitantly with the approach of the westerly trough. This growth is shown by the sequence of blackbody emittance temperature (TBB) analyses in Fig. 7.

4. Discussion

a. Other occurrences

The presence of a warm, dry and convectively suppressed region to the west of tropical cyclones is a common and well documented feature. Even the earliest accounts of tropical cyclones (e.g., Ried, 1838) describe the clear, suppressed cloudiness conditions before the arrival of westward moving storms. Following the advent of meteorological satellites, Fett (1964) showed that a sharp westward edge to the cirrus canopy lay along an upper shear zone between the environment and tropical cyclone outflow. Using rawinsonde observations, Fett showed that this shear zone was as-

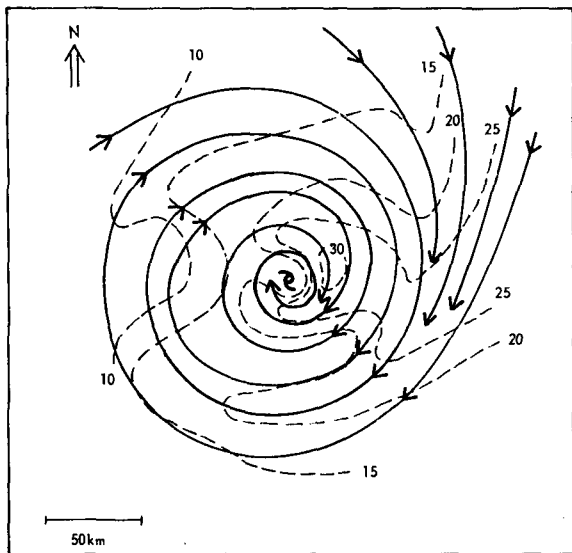


FIG. 4. Composite aircraft reconnaissance observations centered on 2300 on 3 March and at a reference altitude of 540 m (about 950 mb). Isotachs are in $m s^{-1}$.

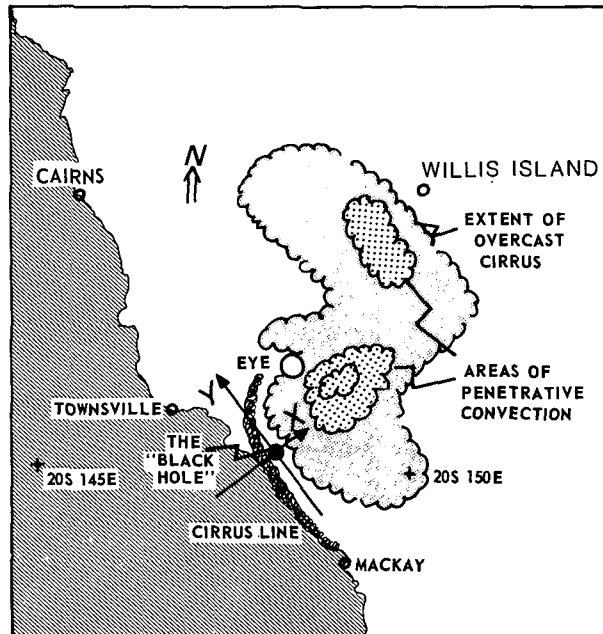


FIG. 6. Schematic of the GMS visible imagery for 0600 on 4 March (Fig. 3) showing the more important features, and the orientation of the xy axis system.

sociated with a presumably subsident annulus of upper tropospheric warming and lower tropospheric drying which moved with the cyclone. He found 250 mb temperature increases of 4–6 K in Hurricane Carla (1961), but also noted that the synoptic network could

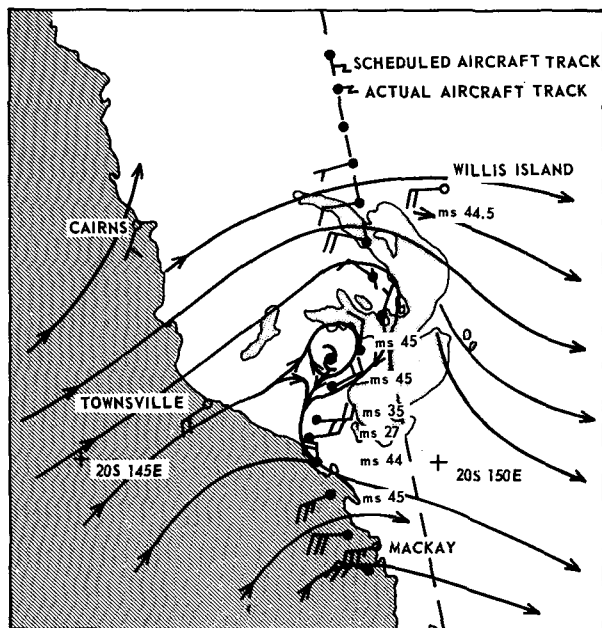


FIG. 5. Track, wind and temperature observations from the aircraft at flight level 370 (~230 mb) and near 0700 GMT. Also included are 200 mb wind observations from 0500 rawin flights at Townsville, Cairns, Willis Island and Mackay, and a schematic of the 0700 PPI display from the Townsville WF44 10 cm radar.

not be expected to fully resolve the effects immediately underneath the narrow (at times 30–40 km wide) shear zone. Holland (1983) obtained similar observations using a compositing approach on southwest Pacific cyclones. He noted 250 mb temperature increases of up to 4 K, together with 500 mb drying of up to $2 g kg^{-1}$ in a band 300–500 mb west and south of these cyclones.

Strong upper tropospheric warming (of up to 13 K at 200 mb) has also been observed downstream of mesoscale convective complexes over the U.S. Great Plains (e.g., Hoxit *et al.*, 1976). Observations and numerical modeling experiments (e.g., Fritsch and Chappell, 1980) indicate that this warming is associated with pronounced mesoscale subsidence driven by the convective complex and that it may be responsible for the subsequent development of mesoscale cyclones at the surface.

Unfortunately, as far as we are aware, no direct observations exist for temperature perturbations of the magnitude of the “black hole”. This is not surprising, given the small-scale transient nature of the perturbation and the paucity of upper tropospheric observations in the vicinity of tropical cyclones. There have been, however, tantalizing glimpses of possible occurrences. W. Shenk (personal communication, 1980) has observed very dry regions on the periphery of tropical cyclones using satellite water vapor channel observations. Presumably, these would be associated with local subsidence and warming. We also examined GMS sat-

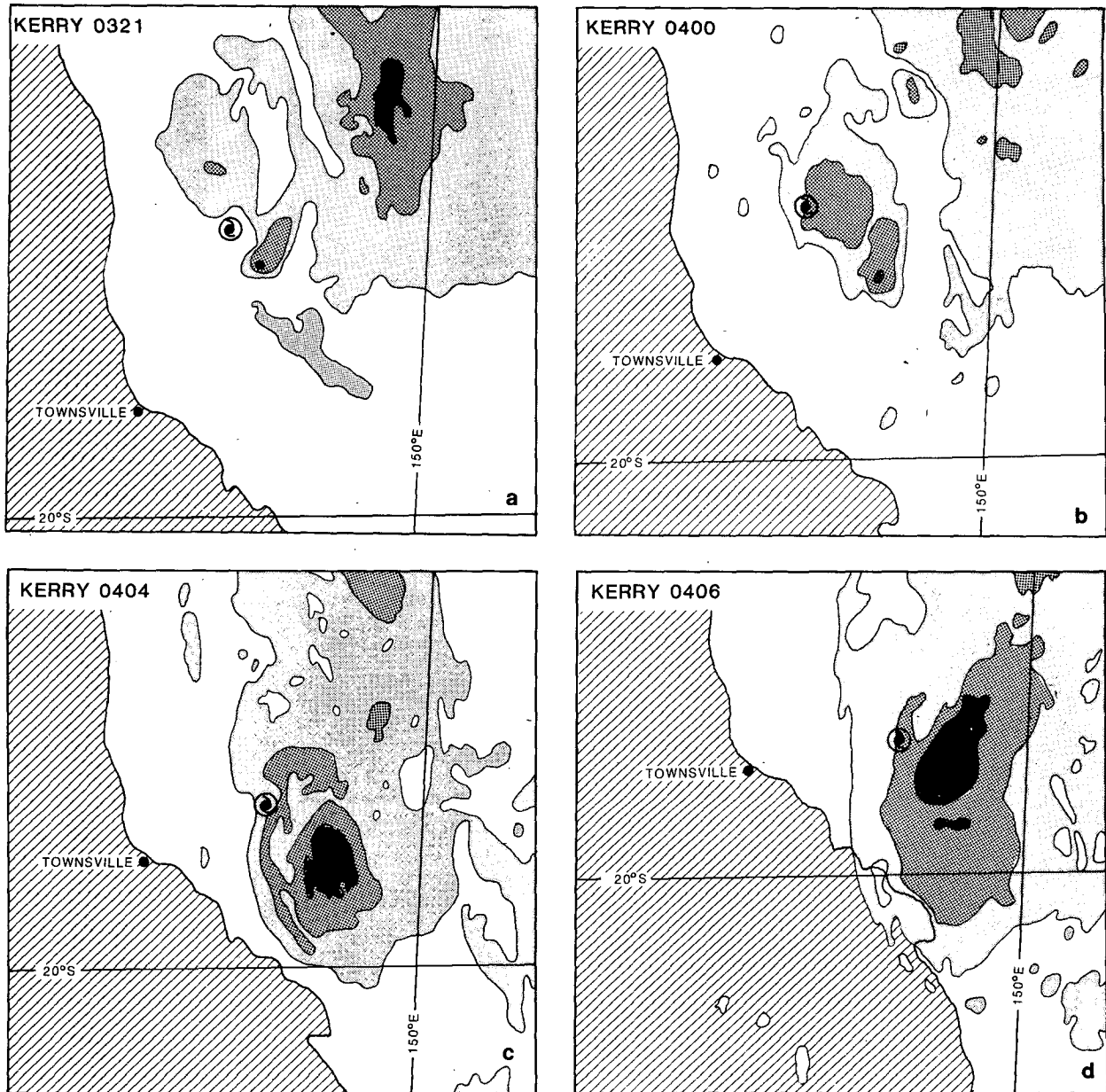


FIG. 7. GMS equivalent blackbody temperature (TBB) analyses for 2100 GMT on 3 March and on 0000, 0400 and 0600 GMT on 4 March. Dark stippling indicates temperatures less than 203 K, medium stippling, 215–203 K and light stippling, 245–215 K.

ellite imagery for all tropical cyclones in the Australian region since 1979 and noted three situations which had similar features to those of Fig. 6. But without direct observations we cannot be certain that temperature perturbations similar to that in Cyclone Kerry occurred.

The TBB analysis for Tropical Cyclone Lena off the West Australian coast in Fig. 8 illustrates the problem. At this time, Lena was interacting with a progressive westerly trough prior to a rapid acceleration to the

southeast. The TBB analysis in Fig. 8 shows a region of active convection with a sharp cutoff on the western edge, a cirrus line separated from this convection by a relatively clear band and even a well defined black hole. In short, very similar features to those for Kerry; all that is needed is a direct observation. Perhaps with more widespread use of satellite derived temperature soundings in the vicinity of tropical cyclones, more objective information will become available in the next few years.

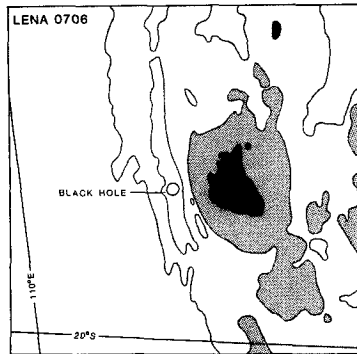


FIG. 8. GMS equivalent blackbody temperature (TBB) analyses for Tropical Cyclone Lena at 0600 on 7 April 1983. Dark stippling indicates temperatures less than 203 K, medium stippling, 215–203 K and light stippling, 245–215 K.

b. Underlying physical processes

Any atmospheric temperature changes must obey the first law of thermodynamics, which may be written as

$$\frac{\partial T}{\partial t} = -\mathbf{V} \cdot \nabla_H T + \omega \left(\alpha - \frac{\partial T}{\partial p} \right) + \frac{Q}{C_p},$$

$$\left[\begin{array}{c} \text{Local} \\ \text{temperature} \\ \text{change} \end{array} \right] = \left[\begin{array}{c} \text{Horizontal} \\ \text{advection} \end{array} \right] + \left[\begin{array}{c} \text{Adiabatic} \\ \text{changes} \end{array} \right] + \left[\begin{array}{c} \text{Diabatic} \\ \text{changes} \end{array} \right] \quad (1)$$

where T is temperature, α specific volume, p pressure, t time, $\omega = dp/dt$ is the vertical wind speed, Q the diabatic heating rate, C_p the specific heat of air at constant pressure and \mathbf{V} the horizontal wind velocity.

The observed temperature perturbation in Fig. 5 cannot be explained by diabatic radiational heating, which is of order $1 \text{ K} (\text{day})^{-1}$. The observed maintenance of a ragged eye over the surface center in Fig. 3, together with the wind observations in Fig. 5 also rule out the possibility of a sheared off, or strongly tilted eye. It is also unlikely that the low coastal topography (of maximum height 1000 m) could have directly affected the upper troposphere to such an extent, though there may have been an indirect affect through modulation of the convective activity. Thus, from Eq. (1), compressional warming in subsiding air is the only process which can conceivably provide the observed temperature increase. This conclusion was also reached by Fett (1964) and by Fritsch (1975) for midlatitude convective complexes. The temperature profile from Willis Island at 2300 on 2 March (Fig. 9), which is representative of the tropical air mass to the southeast and south of the cyclone, indicates that warming of the observed magnitude requires some process which can bring air from the tropopause to

the 250 mb, or lower, level. This then leaves the question of how such a subsidence regime could have been driven.

We suggest that the observed high temperature region is an extreme example of the often observed mesoscale subsidence on the western flank of tropical cyclones that are interacting with a midlatitude trough. The intensity of the temperature perturbation is related to the concomitant rapid growth of the convective complex and impingement of the westerly trough.

If we introduce an x, y, p coordinate system with the horizontal axes oriented as in Fig. 6, then a schematic cross section in the $x-p$ plane at $y = 0$ for 1800 on 3 March will be as shown in Fig. 10. At this time there is little deep penetrative convection (Fig. 7a) and no evidence of any concentrated subsidence warming. The midlatitude trough (Fig. 2a, b) is moving into close proximity but is not yet interacting with the inner core of the cyclone. Upward momentum transports from the cyclonic surface winds (Fig. 4) by convective elements and subsequent detrainment maintain easterly winds in the convective band region, which is overlain by stratospheric easterlies.

At about 0000 on 4 March, an intense convective complex develops to the south of the cyclone eye and penetrates the tropopause, as shown schematically in Fig. 11. That convective cells of the required intensity could occur is indicated by the undilute parcel ascent in Fig. 9. Following the analysis by Fujita (1974) of penetrative convective complexes, the tropopause should be raised as a dome of cold air becomes established over this convective region (see also Fett, 1964, Fig. 11). On the western edge, compensating subsidence will induce a slight downward bulge in the tropopause. Stratospheric easterly momentum will be advected downward in the region and reinforced by outflow from the cold dome and detraining easterlies in the convection. At this stage, the midlatitude trough brings westerlies into a head-on collision. The result is a rapid downward growth of the wave as it converts the kinetic energy of the opposing flows to perturbation potential energy, a process which is described quantitatively below.

Figure 12 shows the situation at the aircraft observation time. Also shown are the Townsville winds at 0600, the stratospheric easterlies over Willis Island and the calculated winds in the cloud region using surface winds and the cloud momentum and detrainment profiles derived by Lee (1982) for tropical cyclone conditions. The actual extent of the downward penetration was not documented, the assumed cutoff at 250 mb is based on available kinetic energy for conversion to potential energy and the information that no marked vertical accelerations were observed by the aircrew. At the boundary between easterly and westerly winds, confluence will have acted as a strong frontogenetic influence and thus produced the observed 18 K in 13

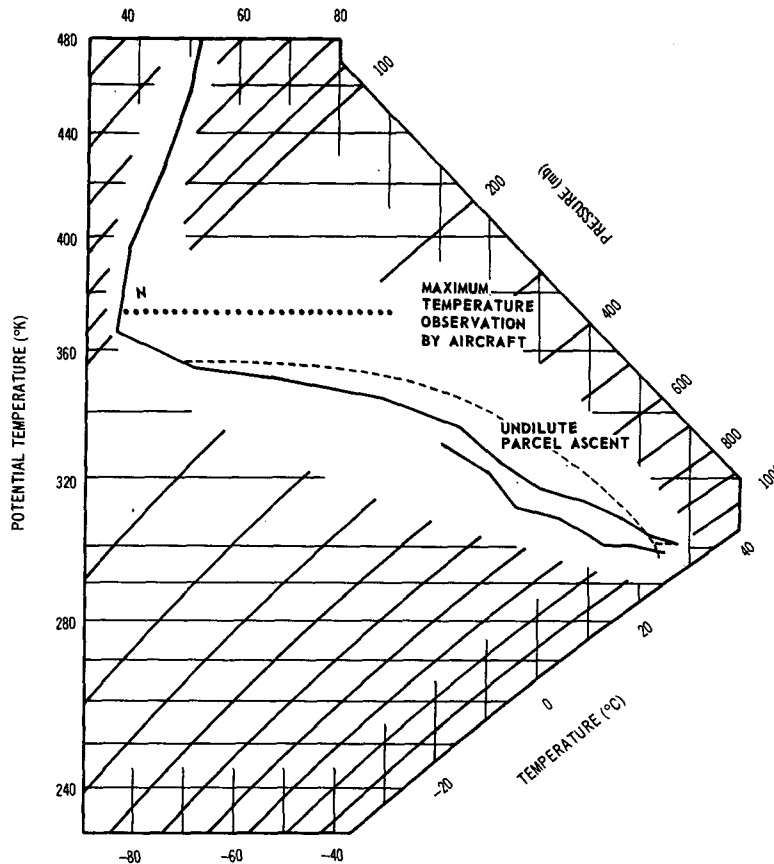


FIG. 9. Temperature profile for Willis Island (see Fig. 6) at 2200 on 2 March. N is the point of neutral equilibrium for a parcel at the aircraft observation point.

km temperature gradient. On the northeastern side, little or no confluence could occur, in agreement with the weaker temperature gradients there.

Here we have considered only two dimensions, along the $x-p$ plane where all our observations are located. It is reasonable to assume that $\partial v/\partial y$ convergence downstream of the convective complex could concentrate the subsidence in the region of the black hole rather than along a two-dimensional "sheet" but we have no quantitative proof that this occurred.

A quantitative estimate of the relevant energetics can be obtained if we assume that the interaction occurs over a narrow zone of convergent easterlies and westerlies of constant speed 15 m s^{-1} (note that the westerlies at the interaction zone are stronger than those for Townsville shown in Fig. 12) and that the growth rate of the disturbance is constant over a 6 h period.

The available potential energy of a parcel of unit mass in the center of the warm core is equal to the work it can do in moving to its point of neutral equi-

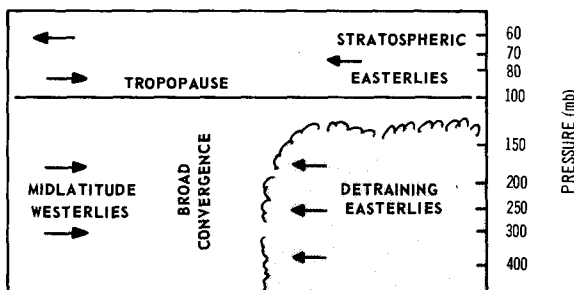


FIG. 10. Schematic $x-p$ cross section along $y = 0$ of the situation for 1800 on 3 March.

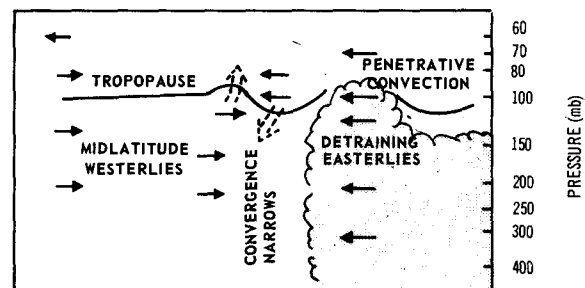


FIG. 11. As in Fig. 10 but for 0000 on 4 March.

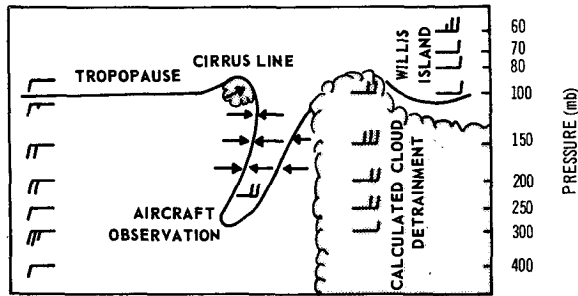


FIG. 12. Schematic x - p cross section along $y = 0$ of the situation for 0600 4 March. The horizontal scale of the downward tropopause extension has been considerably expanded for ease of depiction.

librium (point N in Fig. 9). From elementary parcel theory, the buoyancy force on the parcel will be

$$B = g \left(\frac{T' - T}{T} \right), \tag{2}$$

where g is gravity, T' the parcel temperature and T the environmental temperature. Then the available potential energy is

$$P' = g \int_{z_0}^{z_n} \frac{T' - T}{T} dz, \tag{3}$$

and hence,

$$P' \approx gH \left(\frac{T' - T}{\bar{T}} \right), \tag{4}$$

where z_n is the height of neutral equilibrium, z_0 is the observation height, $H = z_n - z_0$ and the overbar denotes a mean over the layer from z_0 to z_n . For our case at the aircraft observation, $T' - T = 12$ K, $\bar{T} = 220$ K, $H \sim 5$ km. Hence,

$$P' \approx 3 \times 10^3 \text{ m}^2 \text{ s}^{-2}. \tag{5}$$

We have assumed that the process occurs over about 6 h so the time rate of change of potential energy is approximately

$$\frac{\partial P'}{\partial t} \approx 1.5 \times 10^{-1} \text{ m}^2 \text{ s}^{-3}. \tag{6}$$

Now we are assuming a dynamically driven regime in which there are no significant sources or sinks and no advection of P' . Hence the generation of potential energy can only occur by conversion from the kinetic energy of the flow. Thus we require that

$$\frac{dK}{dt} \geq \frac{\partial P'}{\partial t}. \tag{7}$$

If there was no advection of K , then from Eqs. (6) and (7),

$$\frac{dK}{dt} \geq 2 \times 10^{-1} \text{ m}^2 \text{ s}^{-3}. \tag{8}$$

But the local store of kinetic energy is only about $100 \text{ m}^2 \text{ s}^{-2}$ which would be depleted in about 10 min and

could not provide the observed increases in P' . The advective space scale for 10 min is about 10 km. Hence, given a gradient in K of $100 \text{ m}^2 \text{ s}^{-2}$ in 10 km and recalling that kinetic energy is being advected from both sides of the interaction zone, we have

$$\bar{u} \frac{\partial K}{\partial x} \approx 3 \times 10^{-1} \text{ m}^2 \text{ s}^{-3}. \tag{9}$$

Of course not all this advection is available for conversion to perturbation potential energy: some is being converted to perturbation kinetic energy (or wind speed along the negative y direction) as is indicated by the aircraft observed winds at the convergence zone (Fig. 5). However, the convergence must extend over at least 100 km along the y direction so that the conversion to perturbation kinetic energy will be less than $10^{-1} \text{ m}^2 \text{ s}^{-3}$. Thus, this simple model shows that it is possible for the potential energy increase associated with the observed temperature perturbation to have occurred by conversion from the mean kinetic energy of the opposing flow regimes. The narrow predicted 10 km extent of the convergence also agrees very well with the observed 13–20 km extent.

c. Subsequent atmospheric adjustment

Our current understanding of the geostrophic adjustment problem (see Schubert *et al.*, 1980) is that on the mesoscale in tropical latitudes, the mass field tends to adjust to the wind field. Any spontaneous perturbation in the mass field will be largely dissipated by gravity waves and only have a small effect on the wind field. However, the perturbation observed here is so large that even if only, say, ten percent showed up in the wind field, a substantial circulation would result. The question of whether such a circulation response will occur has also been discussed by Gray (1980) for tropical cyclones and by Fritsch and Chappell (1980) for mesoscale convective complexes. Fritsch and Chappell provide strong evidence that mesoscale low formation will occur.

Unfortunately, the region of interest was located over the open ocean and no direct observations could be found to either confirm or deny such a result. The only evidence is supplied by the GMS imagery for 0600 GMT 5 March shown in Fig. 13. The remnants of the eye can still be discerned, but equally discernible is a new, seemingly well developed, lower tropospheric circulation to the southwest in precisely the region of the observed mesoscale warming.

5. Conclusions

A chance commercial aircraft observation of a mesoscale temperature perturbation of 18 K above ambient values near the line of interaction between a tropical cyclone circulation and an encroaching mid-latitude trough has been described. We have shown

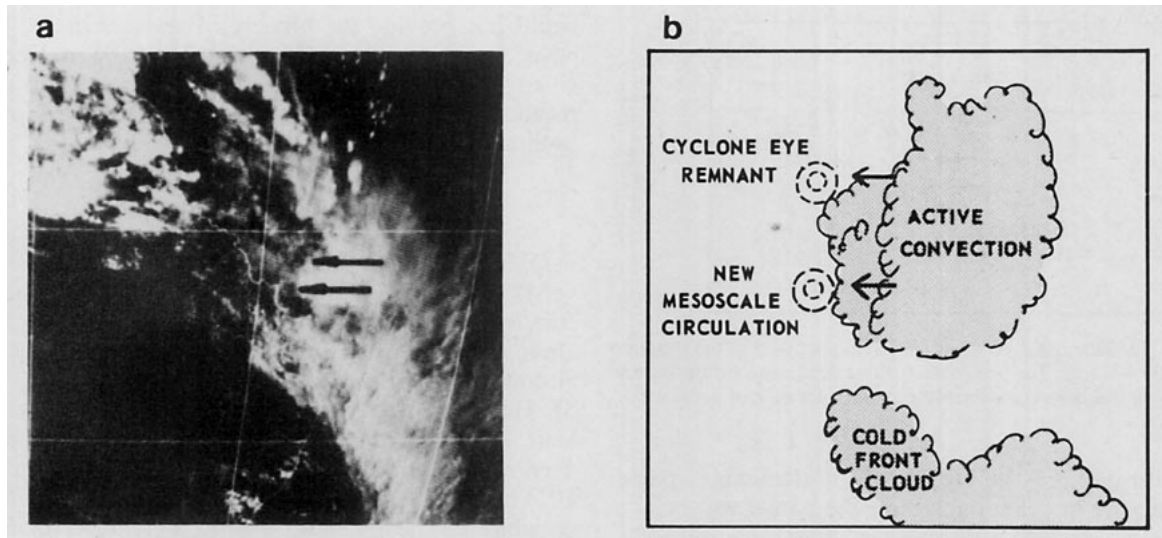


FIG. 13. (a) GMS imagery for 0600 on 5 March and (b) schematic of the important features showing the cyclone eye remnant and new mesoscale circulation.

that the observation, though phenomenal, is consistent with all other available observations. Using a combination of observations and physical reasoning, we have proposed that the warming resulted by the following chain of events: a complex of convective elements on the downstream end of a feeder band penetrated into the stratosphere and generated a perturbation on the tropopause. A dynamic interaction between this convective disturbance and the westerly flow around an impinging midlatitude trough then produced a rapid advection of potentially warm stratospheric air downward. We have further provided evidence that the atmosphere subsequently adjusted at least partially to this warm perturbation to produce a mesoscale circulation.

Acknowledgments. Many thanks to Drs. R. H. Johnson, N. Davidson, P. G. Black and J. M. Fritsch for their helpful comments on this topic, and to B. Brumit and C. Schrandt, A. E. Guymier and L. Marder for their technical assistance. Partial funding for this project was provided by the U.S. Office of Naval Research under Grant N00014-C-0793. This paper is published by permission of the Director of Meteorology, Australia.

REFERENCES

- Broadbridge, L., 1981: The 1978-79 Australian region tropical cyclone season. *Aust. Meteor. Mag.*, **27**, 131-146.
- Fett, R. W., 1964: Aspects of hurricane structure. New model considerations suggested by TIROS and Project Mercury observations. *Mon. Wea. Rev.*, **92**, 43-60.
- Fritsch, J. M., 1975: Cumulus dynamics. Local compensating subsidence and its implications for cumulus parameterisation. *Pure Appl. Geophys.*, **113**, 851-867.
- , and C. F. Chappell, 1980: Numerical prediction of convectively driven mesoscale pressure systems. Part II: Mesoscale model. *J. Atmos. Sci.*, **37**, 1734-1762.
- Fujita, T. T., 1974: Overshooting thunderstorm observed from ATS and Learjet. SMRP Res. Pap. No. 117, Dept. Geophys. Sci., University of Chicago, 29 pp.
- Gray, W. M., 1980: Hurricanes: Their formation, structure and likely role in the tropical circulation. *Meteorology over the Tropical Oceans*, D. B. Shaw, Ed., Royal Meteorological Society, Berkshire RG 121BX, U.K., 155-218.
- Holland, G. J., 1983: Tropical cyclones in the Australian/southwest Pacific region. Atmos. Sci. Pap. No. 363, Colorado State University, Fort Collins, 264 pp.
- Hoxit, L. R., C. F. Chappell and J. M. Fritsch, 1976: Formulation of mesolows or pressure troughs in advance of cumulonimbus clouds. *Mon. Wea. Rev.*, **104**, 1419-1428.
- Lee, C. S., 1982: Vertical rearrangement of tangential momentum in tropical cyclones. Atmos. Sci. Pap., No. 341, Colorado State University, Fort Collins, 78 pp.
- Ried, W., 1838: *The Law of Storms*. John Weale, London, 436 pp.
- Schubert, W. H., J. J. Hack, P. L. Silva Dias and S. R. Fulton, 1980: Geostrophic adjustment in an axisymmetric vortex. *J. Atmos. Sci.*, **37**, 1464-1484.
- Sheets, R. C., and G. J. Holland, 1981: Australian Tropical Cyclones Kerry and Rosa, February-March 1979. NOAA Tech. Memo. ERL AOML-46, National Hurricane Research Laboratory, Coral Gables, FL, 138 pp.